J|A|C|S
ARTICLES
Published on Web 11/19/2003

Continuous Flow Hydroformylation of Alkenes in Supercritical Fluid−Ionic Liquid Biphasic Systems

Paul B. Webb, Murielle F. Sellin, Thulani E. Kunene, Sylvia Williamson, Alexandra M. Z. Slawin, and David J. Cole-Hamilton*

Contribution from the School of Chemistry, University of St. Andrews, St. Andrews, Fife, KY16 9ST, Scotland

Received May 6, 2003; E-mail: djc@st-andrews.ac.uk

Abstract: A process for the hydroformylation of relatively low volatility alkenes (demonstrated for 1-dodecene) in a continuous flow system is described. The catalyst is dissolved in an ionic liquid while the substrate and gaseous reagents are transported into the reactor dissolved in supercritical CO_2, which simultaneously acts as a transport vector for aldehyde products. Decompression of the fluid mixture downstream yields products which are free of both reaction solvent and catalyst. The use of rhodium complexes of triaryl phosphites leads to ligand degradation through reaction of the ionic liquid with water and subsequent attack of the released HF on the phosphite. Sodium salts of sulfonated phosphines are insufficiently soluble in the ionic liquids to obtain acceptable rates, but replacing the sodium by a cation similar to that derived from the ionic liquid, allows good solubility and activity to be obtained. The nature of the ionic liquid is very important in achieving high rates, with 1-alkyl-3-methylimidazolium bis(trifluoromethanesulfonyl)amides giving the best activity if the alkyl chain is at least C_8. Catalyst turnover frequencies as high as 500 h^{-1} have been observed, with the better rates at higher substrate flow rates. Rhodium leaching into the product stream can be as low as 0.012 ppm, except at low partial pressures of CO/H_2, when it is significantly higher. Oxygen impurities in the CO_2 feed can lead to oxidation of the phosphine giving higher rates, lower selectivities to the linear aldehyde, increased alkene isomerization and greater leaching of rhodium. However, it is found that under certain process conditions, the supercritical fluid-ionic liquid (SCF−IL) system can be operated continuously for several weeks without any visible sign of catalyst degradation. Comparisons with commercial hydroformylation processes are provided.

Introduction

Hydroformylation is an important process in the bulk chemicals industry producing more than 6 M tonnes of aldehydes and alcohols per annum for the manufacture of soaps, detergents, and plasticizers.[1,2] Rhodium catalysts show very high activity and good regioselectivity under mild operating conditions for the hydroformylation of alkenes. Triphenylphosphine modified rhodium catalysts are used commercially for the hydroformylation of short chain alkenes (C_2-C_5) but cannot be used for higher alkenes because the catalyst decomposes at temperatures below the boiling point of the aldehyde product making catalyst separation difficult.[1,2] Commercially, this separation problem is overcome by the use of water-soluble catalysts in aqueous−organic two-phase systems. However, this aqueous biphasic approach is only applied to the hydroformylation of propene because the limited solubility of higher olefins in water results in rates that are simply too slow for the process to be commercially viable.[3] Current technology for the synthesis of detergent range alcohols, which produces over 1M tons per annum, is based on less efficient cobalt catalysts, often modified with tertiary phosphines. Cobalt catalysts require more forcing conditions than their rhodium counterparts, a consequence of their lower catalytic activity, and although separation technologies have been developed for Co systems they are by no means simple.[2,4] The selectivity toward linear products in cobalt systems is also often low, although Shell have developed a process based on a phosphine derived from the addition of $C_{20}H_{42}PH_2$ across 1,5-cyclooctadiene, which can give linear/branched ratios (l/b) as high as 10.[5] There are clearly several advantages of working with rhodium compared to cobalt. The development of Rh catalyzed processes, for the hydroformylation of long chain alkenes (C_8-C_{24}), therefore remains one of the biggest challenges in this area.

The catalyst separation problem is not limited to hydroformylation but applies to many homogeneously catalyzed reactions. Although heterogeneous systems may provide the obvious answer to the need for separation, homogeneous catalysts can show much higher activity and selectivity than their heterogeneous counterparts. Nevertheless, the need for separation

(1) Van Leeuwen, P. N. W. M.; Claver, C. *Rhodium Catalysed Hydroformylation*; Kluwer: Dordrecht, 2000.
(2) Frohling, C. D.; Kohlpaintner, C. W. In *Applied Homogeneous Catalysis with Organometallic Compounds*; Cornils, B., Herrmann, W. A., Ed.; VCH: Weinheim, 1996; Vol. 1, pp 27−104.
(3) Cornils, B. In *Applied Homogeneous Catalysis with Organometallic Compounds*; Cornils, B., Herrmann, W. A., Ed.; VCH: Weinheim, 1996; Vol. 1, pp 577−600.
(4) Cornils, B. In *New Synthesis with Carbon Monoxide*; Falbe, J., Ed.; Springer-Verlag: Berlin, 1980.
(5) Mullineaux, R. D.; Slaugh, L. H. U.S. Patents 3,239,569 and 3,269,570, 1966.

10.1021/ja035967s CCC: $25.00

sometimes prevents the commercialization of otherwise very attractive homogeneous systems. This has prompted extensive research into methods which combine the ease of catalyst recovery associated with heterogeneous systems with the more desirable activity and selectivity obtained with homogeneous catalysts.[6,7] These approaches can be divided into two main categories involving either (i) anchoring the catalyst to a soluble or insoluble support (heterogenisation), or (ii) dissolving the catalyst in a solvent which is immiscible with the reaction product under certain conditions (biphasic). We have been exploring aqueous biphasic,[8] fluorous biphasic,[9,10] dendrimer anchored,[11−15] and supported catalysts,[16,17] as well as the use of supercritical fluids[18−21] as methods for overcoming the separation problem. All of these approaches, however, suffer from the disadvantage that some of the reaction medium must be removed from the bulk before catalyst separation can be effected. As a consequence, not all of the catalyst is involved in the reaction at all times, and perhaps more importantly, the conditions for catalyst separation can be very different from those of the reaction such that catalyst decomposition may still occur. An ideal system would enable continuous operation with separation under conditions identical to those of the reaction itself so that all of the catalyst remains in its active state at all times. The ability to afford reaction and separation under a single set of conditions would not only reduce the problems of catalyst deactivation but would also have a considerable effect on the size of reactor needed for a given product throughput. Reductions in reactor volumes then offer further advantages in terms of safety (e.g., smaller volumes of inflammable gases) and reduced capital costs.

Following the pioneering work of Brennecke,[22,23] we recently reported an example of a homogeneously catalyzed, continuous flow process for products which are of too low a volatility to be removed by direct distillation from the reaction mixture. The process involved dissolving an ionic catalyst in an ionic liquid and using supercritical CO_2 ($scCO_2$) as a transport vector for both gaseous and liquid substrates and products.[24] This biphasic approach relies on Brennecke's important observation that CO_2 is highly soluble in ionic liquids (up to 0.6 mole fraction), whereas the gas rich phase remains free of dissolved ionic liquid.[22] Brennecke later demonstrated that a wide range of organics, of varying chemical functionality, could be extracted from ionic liquids using $scCO_2$ while the ionic liquid itself is completely retained.[23] The gaslike mass transport characteristics of a supercritical fluid and its complete miscibility with permanent gases coupled with the liquidlike ability to dissolve organic compounds of low to medium polarity makes it an ideal transport vector. The SCF−IL biphasic system enables continuous operation and differs from other biphasic systems in that one of the phases is a dense gas. Thus, unlike many liquid−liquid biphasic systems, the separation of product from catalyst and reaction solvent can be carried out under a single set of conditions with the advantage that all of the catalyst remains in its active state at all times. Furthermore, decompression of the gaseous mixture downstream yields products which are free from reaction solvent, thereby removing the necessity for additional purification by distillation.

The work of Brennecke has prompted an increasing interest into the combination of ionic liquid and SCF technologies. Reactions including the hydrogenation of 1-decene[25] and the asymmetric hydrogenation of tiglic acid[26] have both been performed successfully in ionic liquids followed by supercritical fluid extraction of the reaction products. More recently, the continuous flow approach using CO_2 and ionic liquids has been applied to the codimerization of ethene and styrene,[27] (although the temperature was below the critical temperature for CO_2) the Wacker oxidation of alkenes,[28] the reaction between alkenes and CO_2 [29] and reactions using enzymes.[30,31] A short review of the SCF−IL biphasic approach has recently appeared.[32]

Materials and Methods

Elemental analyses were performed by the University of St. Andrews Microanalysis service on a Carlo Erba 1110 CHNS analyzer. NMR spectra were recorded on a Varian 300 spectrometer using protio impurities of the deuterated solvent as a reference for ^1H and ^{13}C chemical shifts, with tertramethylsilane at 0 ppm. ^{31}P chemical shifts are reported to high frequency of external 85% H_3PO_4. IR spectra were recorded on a Nicolet Avatar 300 FT-IR spectrometer fitted with an MCT-A detector. All reagents were used as received (Aldrich) without further purification with the exception of liquid substrates for catalytic experiments which were dried and degassed according to literature methods. 1-Dodecene was purified further by distillation through a high efficiency column.

Gas chromatographic analyses of the product mixtures were carried out on a Hewlett-Packard 5890 series gas chromatograph equipped with

(6) Tzschucke, C. C.; Markert, C.; Bannwarth, W.; Roller, S.; Hebel, A.; Haag, R. *Angew. Chem., Int. Ed.* **2002**, *41*, 3964−4000.
(7) Cole-Hamilton, D. J. *Science* **2003**, *299*, 1702.
(8) Borowski, A. F.; Cole-Hamilton, D. J.; Wilkinson, G. *Nouv. J. Chem.* **1978**, *2*, 137.
(9) Foster, D. F.; Adams, D. J.; Gudmunsen, D.; Stuart, A. M.; Hope, E. G.; Cole-Hamilton, D. J. *Chem. Commun.* **2002**, 916−916.
(10) Foster, D. F.; Gudmunsen, D.; Adams, D. J.; Stuart, A. M.; Hope, E. G.; Cole-Hamilton, D. J.; Schwarz, G. P.; Pogorzelec, P. *Tetrahedron* **2002**, *58*, 3901−3910.
(11) Ropartz, L.; Morris, R. E.; Schwarz, G. P.; Foster, D. F.; Cole-Hamilton, D. J. *Inorg. Chem. Commun.* **2000**, *3*, 714−717.
(12) Ropartz, L.; Foster, D. F.; Morris, R. E.; Slawin, A. M. Z.; Cole-Hamilton, D. J. *J. Chem. Soc.-Dalton Trans.* **2002**, 1997−2008.
(13) Ropartz, L.; Haxton, K. J.; Foster, D. F.; Morris, R. E.; Slawin, A. M. Z.; Cole-Hamilton, D. J. *J. Chem. Soc.-Dalton Trans.* **2002**, 4323−4334.
(14) Ropartz, L.; Morris, R. E.; Foster, D. F.; Cole-Hamilton, D. J. *J. Mol. Catal. A-Chem.* **2002**, *182*, 99−105.
(15) Ropartz, L.; Morris, R. E.; Foster, D. F.; Cole-Hamilton, D. J. *Chem. Commun.* **2001**, 361−362.
(16) De Blasio, N.; Tempesti, E.; Kaddouri, A.; Mazzocchia, C.; Cole-Hamilton, D. J. *J. Catal.* **1998**, *176*, 253−259.
(17) De Blasio, N.; Wright, M. R.; Tempesti, E.; Mazzocchia, C.; Cole-Hamilton, D. J. *J. Organomet. Chem.* **1998**, *551*, 229−234.
(18) Bach, I.; Cole-Hamilton, D. J. *Chem. Commun.* **1998**, 1463−1464.
(19) Sellin, M. F.; Cole-Hamilton, D. J. *J. Chem. Soc.-Dalton Trans.* **2000**, *11*, 1681−1683.
(20) Sellin, M. F.; Bach, I.; Webster, J. M.; Montilla, F.; Rosa, V.; Aviles, T.; Poliakoff, M.; Cole-Hamilton, D. J. *J. Chem. Soc.-Dalton Trans.* **2002**, 4569−4576.
(21) Sowden, R. J.; Sellin, M. F.; De Blasio, N.; Cole-Hamilton, D. J. *Chem. Commun.* **1999**, 2511−2512.
(22) Blanchard, L. A.; Hancu, D.; Beckman, E. J.; Brennecke, J. F. *Nature* **1999**, *399*, 28−29.
(23) Blanchard, L. A.; Brennecke, J. F. *Ind. Eng. Chem. Res.* **2001**, *40*, 287−292.
(24) Sellin, M. F.; Webb, P. B.; Cole-Hamilton, D. J. *Chem. Commun.* **2001**, 781−782.
(25) Liu, F. C.; Abrams, M. B.; Baker, R. T.; Tumas, W. *Chem. Commun.* **2001**, 433−434.
(26) Brown, R. A.; Pollet, P.; McKoon, E.; Eckert, C. A.; Liotta, C. L.; Jessop, P. G. *J. Am. Chem. Soc.* **2001**, *123*, 1254−1255.
(27) Bosmann, A.; Francio, G.; Janssen, E.; Solinas, M.; Leitner, W.; Wasserscheid, P. *Angew. Chem., Int. Ed.* **2001**, *40*, 2697−2699.
(28) Hou, Z. S.; Han, B. X.; Gao, L.; Jiang, T.; Liu, Z. M.; Chang, Y. H.; Zhang, X. G.; He, J. *New J. Chem.* **2002**, *26*, 1246−1248.
(29) Kawanami, H.; Sasaki, A.; Matsui, K.; Ikushima, Y. *Chem. Commun.* **2003**, 896−897.
(30) Lozano, P.; de Diego, T.; Carrie, D.; Vaultier, M.; Iborra, J. L. *Chem. Commun.* **2002**, 692−693.
(31) Reetz, M. T.; Wiesenhofer, W.; Francio, G.; Leitner, W. *Chem. Commun.* **2002**, 992−993.
(32) Dzyuba, S. V.; Bartsch, R. A. *Angew. Chem., Int. Ed.* **2003**, *42*, 148−150.

both a flame ionization detector (GCFID for quantitative analyses) and a mass selective detector (GCMS for qualitative analyses). The gas chromatograph was interfaced with a Hewlett-Packard Chemstation for the determination of peak areas by electronic integration. The GCMS and GCFID methods employed a Supelco Meridian MDN-35 low polarity, cross-linked phase comprised of a (35% phenyl)-methylpolysiloxane fused silica capillary column (30 m × 0.25 mm × 0.25 μm).

Rhodium analyses of recovered fractions were measured by inductively coupled mass spectrometry (ICPMS) on an Agilent 7500a instrument. The instrument was modified for direct analyses of the organic fractions by using O_2 as a makeup gas to prevent carbon deposition on the sample and skimmer cones. Platinum cones were used together with a self-aspirating nebulizer held at −5 °C. Samples were diluted by 10% in a mixture of xylene and toluene (50:50) and ion counts were referenced against calibration curves obtained from standard solutions of [Rh(acac)(CO)$_2$] (acacH is 2,4-dimethylpentanedione) in xylene/toluene (50:50). Standard solutions were run intermittently between samples to ensure that there were no drifts in instrument response and that the rate of aspiration was constant.

A. Syntheses. (1) 1-Alkyl-3-methylimidazolium Chloride. *N*-Methyl imidazole and a 1.3-fold excess of the corresponding chloroalkane were refluxed at 70 °C for 3 days. After cooling, the upper layer was discarded and the IL was washed with ethyl acetate and then dried in vacuo at 50 °C for 5 h. The product was then dissolved in water and stirred at room temperature in the presence of activated charcoal for 24 h. The solution was filtered through diatomaceous earth, and again dried in vacuo to yield **(1)** as a colorless liquid in all cases except the propyl, butyl, and decyl analogues which crystallized at room temperature as white solids. The imidazole chlorides were analyzed by ^{1}H NMR and compared to literature data. NMR data is provided for those compounds which have not yet been fully characterized. We were unable to obtain accurate microanalysis for the imidazole chlorides because of their hygroscopic nature.

(1a) 1-Propyl-3-methylimidazolium Chloride [PrMIM]Cl. ^{1}H NMR (300 MHz, CD_2Cl_2, 298 K): δ = 0.67 (3H, t, CH_3), 1.68 (2H, sext, C*H*$_2$CH$_3$), 3.85 (3H, s, NCH_3), 4.09 (2H, t, NCH_2), 7.71, 7.73 (2H, 2 × t, NC(H)C(H)N), 10.29 (1H, s, NC(H)N) ppm. ^{13}C NMR (75.4 MHz, CD_2Cl_2, 298 K): δ = 137.2 (s, NCN), 123.4, 122.1 (2 × s, NCCN), 50.6 (s, NCH_2), 35.9 (d, NCH_3), 23.3 (s, CH_2), 10.2 (s, CH_3) ppm.

(1b) 1-Octyl-3-methylimidazolium Chloride [OctMIM]Cl. ^{1}H NMR (300 MHz, CD_2Cl_2, 298 K): δ = 0.81 (3H, t, CH_3), 1.21−1.27 (10H, m, CH_2), 1.85 (2H, pent, NCH_2CH_2), 4.03 (3H, s, NCH_3), 4.26 (2H, t, NCH_2), 7.48, 7.63 (2H, 2 × t, NC(H)C(H)N), 10.64 (1H, s, NC(H)N) ppm. ^{13}C NMR (75.4 MHz, CD_2Cl_2, 298 K): δ = 138.4 (s, NCN), 123.9, 122.3 (2 × s, NCCN), 50.2 (s, NCH_2), 36.7 (s, NCH_3), 32.0, 30.6, 29.4, 29.3, 26.6, 22.9 (6 × s, CH_2), 14.2 (s, CH_3) ppm.

(1c) 1-Decyl-3-methylimidazolium Chloride [DecMIM]Cl. ^{1}H NMR (300 MHz, CD_2Cl_2, 298 K): δ = 0.87 (3H, t, CH_3), 1.26−1.32 (14H, m, CH_2), 1.88 (2H, pent, NCH_2CH_2), 4.06 (3H, s, NCH_3), 4.28 (2H, t, NCH_2), 7.28, 7.36 (2H, 2 × t, NC(H)C(H)N), 10.39 (1H, s, NC(H)N) ppm. ^{13}C NMR (75.4 MHz, CD_2Cl_2, 298 K): δ = 138.7 (s, NCN), 123.7, 122.1 (2 × s, NCCN), 50.6 (s, NCH_2), 37.0 (s, NCH_3), 32.4, 30.8, 30.0, 29.9, 29.8, 29.6, 26.8, 23.2 (8 × s, CH_2), 14.4 (s, CH_3) ppm.

(1d) 1-Butyl-2,3-dimethylimidazolium Chloride [BDMIM]Cl. ^{1}H NMR (300 MHz, CD_2Cl_2, 298 K): δ = 0.95 (3H, t, CH_3), 1.37 (2H, sext, C*H*$_2$CH$_3$), 1.78 (2H, pent, NCH_2CH_2), 2.74 (3H, s, $NC(CH_3)N$), 3.99 (3H, s, NCH_3), 4.19 (2H, t, NCH_2), 7.58, 7.87 (2H, 2 × d, NC(H)C(H)N) ppm. ^{13}C NMR (75.4 MHz, CD_2Cl_2, 298 K): δ = 144.3 (s, NCN), 123.7, 121.7 (2 × s, NCCN), 49.1 (s, NCH_2), 36.2 (s, NCH_3), 32.3, 20.1 (2 × s, CH_2), 13.8 (s, $NC(CH_3)N$), 10.8 (s, CH_3) ppm.

(2) 1-Alkyl-3-methylimidazolium Hexafluorophosphate. Preparations of the imidazolium PF_6 salts were carried out as follows: A solution of sodium hexafluorophosphate in water was added to an aqueous solution of the corresponding imidazolium chloride in stoichiometric quantities. After stirring at room temperature for 24 h, the aqueous phase was decanted and the ionic liquid washed with water until the washings were free from chloride. The ionic liquid was then dissolved in acetone and stirred in the presence of activated charcoal for 24 h. The solution was filtered through diatomaceous earth and the solvent removed in vacuo. The ionic liquid was again washed with water and dried in vacuo to yield **(2)** as a colorless liquid. The imidazole hexafluorophosphates were analyzed by ^{1}H NMR and compared to literature data.

(2a) 1-Butyl-2,3-dimethylimidazolium Hexafluorophosphate [BDMIM]PF$_6$. 1-butyl-2,3-dimethylimidazolium hexafluorophosphate was similarly prepared using 1,2-dimethylimidazolium chloride. Elemental analysis calcd. for $C_9H_{17}N_2PF_6$: C 36.25 H 5.75 N 9.39; found: C 36.38 H 5.68 N 9.36. ^{1}H NMR (300 MHz, CD_2Cl_2, 298 K): δ = 0.98 (3H, t, CH_3), 1.39 (2H, sext, C*H*$_2$CH$_3$), 1.81 (2H, pent, NCH_2CH_2), 2.60 (3H, s, $NC(CH_3)N$), 3.80 (3H, s, NCH_3), 4.05 (2H, t, NCH_2), 7.18, 7.21 (2H, 2 × d, NC(H)C(H)N) ppm. ^{13}C NMR (75.4 MHz, CD_2Cl_2, 298K): δ = 144.3 (s, NCN), 122.9, 121.3 (2 × s, NCCN), 49.0 (s, NCH_2), 35.6 (s, NCH_3), 32.0, 19.6 (2 × s, CH_2), 13.7 (s, $NC(CH_3)N$), 9.7 (s, CH_3) ppm.

(3) 1-Alkyl-3-methylimidazolium Bis(trifluoromethanesulfonyl)-amide. The bis(trifluoromethanesulfonyl)amide salts were similarly prepared using N-lithio bis(trifluoromethanesulfonyl)amide for the salt exchange reaction. Full analysis is provided for the imidazole sulfonyl amides which have not yet been fully characterized.

(3a) 1-Octyl-3-methylimidazolium Bis(trifluoromethanesulfonyl)-amide [OctMIM]NTf$_2$. Elemental analysis calcd. for $C_{14}H_{23}O_4N_3S_2F_6$: C 35.37 H 4.87 N 8.84; found: C 35.00 H 5.52 N 9.16. ^{1}H NMR (300 MHz, CD_2Cl_2, 298 K): δ = 0.88 (3H, t, CH_3), 1.27−1.33 (10H, m, CH_2), 1.86 (2H, pent, NCH_2CH_2), 3.92 (3H, s, NCH_3), 4.15 (2H, t, NCH_2), 7.30, 7.31 (2H, 2 × s, NC(H)C(H)N) 8.61 (1H, s, NC(H)N) ppm. ^{13}C NMR (75.4 MHz, CD_2Cl_2, 298 K): δ = 136.3 (s, NCN), 124.3, 122.9 (2 × d, NCCN), 120.4 (q, CF_3, J_{CF} = 321 Hz), 50.8 (s, NCH_2), 36.8 (s, NCH_3), 32.2, 30.6, 29.5, 29.3, 26.6, 23.1 (6 × s, CH_2), 14.3 (s, CH_3) ppm.

(3b) 1-Decyl-3-methylimidazolium Bis(trifluoromethanesulfonyl)-amide [DecMIM]NTf$_2$. Elemental analysis calcd for $C_{16}H_{27}O_4N_3S_2F_6$: C 38.17 H 5.40 N 8.35; found: C 37.87 H 5.84 N 8.88. ^{1}H NMR (300 MHz, CD_2Cl_2, 298 K): δ = 1.00 (3H, t, CH_3), 1.40−1.46 (14H, m, CH_2), 1.99 (2H, pent, NCH_2CH_2), 4.05 (3H, s, NCH_3), 4.28 (2H, t, NCH_2), 7.42, 7.43 (2H, 2 × d, NC(H)C(H)N), 8.75 (1H, s, NC(H)N) ppm. ^{13}C NMR (75.4 MHz, CD_2Cl_2, 298 K): δ = 136.4 (s, NCN), 124.2, 122.8 (2 × s, NCCN), 120.4 (q, CF_3, J_{CF} = 321 Hz), 50.9 (s, NCH_2), 36.9 (s, NCH_3), 32.4, 30.6, 30.0, 29.9, 29.8, 29.4, 26.6, 23.1 (8 × s, CH_2), 14.4 (s, CH_3) ppm.

(4) 1-Propyl-3-methylimidazolium Diphenyl(3-sulfonatophenyl)-phosphine ([PrMIM][TPPMS]). [PrMIM]Cl (**1a**) (14.31 g, 89.1 mmol) was added dropwise to a rapidly stirred solution of sodium diphenyl-(3-sulfonatophenyl)phosphine dihydrate[33] (25.74 g, 64.3 mmol) in THF, resulting in immediate formation of a fine white precipitate. The solution was stirred at room temperature for a further 24 h, filtered through diatomaceous earth, and the solvent removed in vacuo. The resulting residue was taken up into dichloromethane, again filtered, and the solvent removed in vacuo. The crude product, which contains an excess of the imidazolium chloride, was left at −10 °C to afford **(4)** as colorless rhomboidal crystals (15.28 g, 32.8 mmol, 50.9%) mpt 88−90 °C. Elemental analysis calcd for $C_{25}H_{27}O_3N_2PS$: C 64.36 H 5.83 N 6.00; found: C 64.42 H 5.64 N 6.14. IR (CsI): $\tilde{\nu}$ = 3156 (w), 3097 (m), 3047 (m), 2969 (w), 2883 (w), 1580 (m), 1479 (m), 1461 (w), 1434 (m), 1394 (w), 1309 (w), 1202 (s, br), 1139 (m), 1091 (m), 1070 (w), 1031 (s), 995 (w), 890 (w), 796 (m), 784 (m), 749 (s), 698 (s), 673 (m), 617 (s), 595 (w), 555 (w) cm^{-1}. ^{1}H NMR (300 MHz, CD_2Cl_2, 298 K): δ = 0.99 (3H, t, CH_3), 1.92 (2H, sext, C*H*$_2$CH$_3$), 3.97 (3H, s,

(33) Joó, F.; Kovács, J.; Kathó, A.; Bényei, A. C.; Decuir, T.; Dahrensbourg, D. J. **1998**, *32*, 2.

NCH_3), 4.20 (2H, t, NCH_2), 7.43 (14H, m, $Ph_2PC_6H_4SO_3$), 7.92, 7.96 (2H, 2 × d, NC(H)C(H)N), 9.71 (1H, s, NC(H)N) ppm. ^{13}C NMR (75.4 MHz, CD_2Cl_2, 298 K): δ = 148.1 (d, CSO_3, J_{pc} = 6.9 Hz), 138.2 (s, NCN), 138.0 (d, *ipso*-C_6H_5, J_{pc} = 12.7 Hz), 137.5 (d, *ipso*-$C_6H_4SO_3$, J_{pc} = 11.5 Hz), 134.6 (d, *o*-$C_6H_4SO_3$, J_{pc} = 14.9 Hz), 134.2 (d, *o*-C_6H_5, J_{pc} = 19.6 Hz), 131.3 (d, *o*-*C*CSO_3, J_{pc} = 25.3 Hz), 129.3 (s, *p*-C_6H_5), 129.0 (d, *m*-C_6H_5, J_{pc} = 6.9 Hz), 128.8 (d, *m*, $C_6H_4SO_3$, J_{pc} = 5.8 Hz), 126.8 (s, *p*-$C_6H_4SO_3$), 123.8, 122.4 (2 × s, NCCN), 51.6 (s, NCH_2), 36.5 (s, NCH_3), 23.9 (s, CH_2), 10.9 (s, CH_3) ppm. ^{31}P NMR (121.4 MHz, CD_2Cl_2, 298 K) δ = −3.90.

(5) 1-Butyl-3-methylimidazolium Diphenyl(3-sulfonatophenyl)-phosphine Monohydrate ([BMIM][TPPMS]·H_2O). A solution of 1-butyl-3-methylimidazolium chloride (1.00 g, 5.73 mmol) in methanol (ca. 5 cm^3) was added to a rapidly stirred solution of sodium diphenyl-(3-sulfonatophenyl)phosphine dihydrate (4.01 g, 10.02 mmol) in THF (50 cm^3). The solution was stirred at room temperature for 24 h, filtered through diatomaceous earth, and the solvent removed in vacuo. The resulting residue was taken up into dichloromethane, again filtered through diatomaceous earth, and the solvent removed in vacuo. The crude product, which contains excess phosphine, was washed with propan-2-ol (3 × 20 cm^3), the washings were combined and the solvent removed in vacuo. The resulting residue was dissolved in acetone and layered with diethyl ether to yield **(5)** (1.42 g, 2.96 mmol, 51.6%) as colorless crystals on standing. Elemental analysis calcd. for $C_{26}H_{31}O_4N_2PS$: C 62.64 H 6.27 N 5.62; found: C 62.45 H 6.37 N 5.66. IR (CsI): $\tilde{\nu}$ = 3156 (w), 3097 (m), 3047 (m), 2969 (w), 2883 (w), 1580 (m), 1479 (m), 1461 (w), 1434 (m), 1394 (w), 1309 (w), 1202 (s, br), 1139 (m), 1091 (m), 1070 (w), 1031 (s), 995 (w), 890 (w), 796 (m), 784 (m), 749 (s), 698 (s), 673 (m), 617 (s), 595 (w), 555 (w) cm^{-1}. ^1H NMR (300 MHz, CD_2Cl_2, 298 K): δ = 0.98 (3H, t, CH_3), 1.35 (2H, sext, CH_2CH_3), 1.82 (2H, pent, NCH_2CH_2), 3.90 (3H, s, NCH_3), 4.18 (2H, t, NCH_2), 7.30 (14H, m, $Ph_2PC_6H_4SO_3$), 7.88, 7.97 (2H, 2 × d, NC(H)C(H)N), 9.67 (1H, s, NC(H)N) ppm. ^{13}C NMR (75.4 MHz, CD_2Cl_2, 298 K): δ = 146.8 (d, CSO_3, J_{pc} = 6.9 Hz), 138.5 (s, NCN), 138.0 (d, *ipso*-C_6H_5, J_{pc} = 12.7 Hz), 137.5 (d, *ipso*-$C_6H_4SO_3$, J_{pc} = 11.5 Hz), 134.9 (d, *o*-$C_6H_4SO_3$, J_{pc} = 12.6 Hz), 134.2 (d, *o*-C_6H_5, J_{pc} = 19.6 Hz), 131.6 (d, *o*-*C*CSO_3, J_{pc} = 27.7 Hz), 129.4 (s, *p*-C_6H_5), 129.0 (d, *m*-C_6H_5, J_{pc} = 6.9 Hz), 128.8 (d, *m*, $C_6H_4SO_3$, J_{pc} = 5.8 Hz), 127.2 (s, *p*-$C_6H_4SO_3$), 123.6, 122.0 (s × 2, NCCN), 50.2 (s, NCH_2), 36.8 (s, NCH_3), 32.4, 19.9 (2 × s, CH_2), 13.7 (s, CH_3) ppm. ^{31}P NMR (121.4 MHz, CD_2Cl_2, 298 K) δ = −3.90.

(6) 1-Butyl-2,3-dimethylimidazolium Diphenyl(3-sulfonatophenyl)phosphine ([TPPMS][BDMIM]). A solution of 1-butyl-2,3-dimethylimidazolium chloride (1d) (0.47 g, 2.47 mmol) and sodium diphenyl-(3-sulfonatophenyl)phosphine dihydrate (1.00 g, 2.50 mmol) in acetone (ca. 40 cm^3) was stirred at room temperature for 24 h. The solution was then filtered through a plug of diatomaceous earth, and the solvent removed from the filtrate in vacuo. The residue was washed with acetone and dried in vacuo to yield **(6)** (0.80 g, 1.62 mmol, 65.5%) as a fine white powder. Elemental analysis calcd. for $C_{27}H_{31}O_3N_2PS$: C 65.57 H 6.32 N 5.66; found: C 65.58 H 6.40 N 5.57. IR (Nujol): $\tilde{\nu}$ = 3160 (w), 3120 (m), 3047 (m), 2721 (w), 1584 (m), 1539 (m), 1377 (s), 1310 (w), 1263(w) 1205 (s, br), 1136 (m), 1089 (m), 1070 (w), 1029 (s), 993 (w), 908 (w), 796 (m), 784 (m), 761 (s), 746 (s) 693 (s), 674 (m), 659 (w) 617 (s), 595 (w), 555 (w) cm^{-1}. ^1H NMR (300 MHz, $CDCl_3$, 298 K): δ = 0.84 (3H, t, CH_3), 1.24 (2H, sext, CH_2CH_3), 1.62 (2H, pent, NCH_2CH_2), 2.52 (3H, s, $NC(CH_3)N$), 3.71 (3H, s, NCH_3), 3.95 (2H, t, NCH_2), 7.27 (14H, m, $Ph_2PC_6H_4SO_3$), 7.80, 7.87 (2H, 2 × d, NC(H)C(H)N) ppm. ^{13}C NMR (75.4 MHz, $CDCl_3$, 298 K): δ = 147.8 (d, CSO_3, J_{pc} = 6.9 Hz), 143.9 (s, NCN), 137.6 (d, *ipso*-C_6H_5, J_{pc} = 11.5 Hz), 137.1 (d, *ipso*-$C_6H_4SO_3$, J_{pc} 10.8 = Hz), 134.3 (d, *o*-$C_6H_4SO_3$, J_{pc} = 13.0 Hz), 133.9 (d, *o*-C_6H_5, J_{pc} = Hz), 131.5 (d, *o*-*C*CSO_3, J_{pc} = Hz), 128.9 (s, *p*-C_6H_5), 128.6 (d, *m*-C_6H_5, J_{pc} = Hz), 128.8 (d, *m*, $C_6H_4SO_3$, J_{pc} = Hz), 126.8 (s, *p*-$C_6H_4SO_3$), 123.0, 121.0 (s × 2, NCCN), 48.3 (s, NCH_2), 35.4 (s, NCH_3), 31.5, 19.5 (2 × s, CH_2), 13.4 (s, $NC(CH_3)N$), 9.8 (s, CH_3) ppm. ^{31}P NMR (121.4 MHz, DMSO, 298 K) δ = −4.46.

B. Catalytic Reactions. 1. Batch and Semi-continuous Reactions. All batch and semi-continuous reactions were performed in a Hastelloy reactor (36 or 48 cm^3) fitted with a magnetically driven stirrer, thermocouple, pressure transducer, and gas inlet and outlet valves. For semi-continuous operation, the reaction autoclave was coupled to a second autoclave fitted with an expansion valve at the inlet port. The second autoclave was also fitted with a thermocouple and pressure transducer.

2. Batch Reactions of 1-Dodecene. [$Rh(acac)(CO)_2$] (46.8 mg, 0.18 mmol) was weighed into an autoclave (30 cm^3) fitted with a magnetically driven stirrer. The autoclave was purged with CO/H_2 and then charged with a solution of [PrMIM][TPPMS] **(4)** (1.31 g, 2.81 mmol) in the ionic liquid (12 cm^3), again under a CO/H_2 purge. The autoclave was pressurized with CO/H_2 (1:1, 40 bar) and heated to 100 °C with rapid stirring. The catalyst solution was stirred for 1 h at 1100 rpm to allow for the formation of active catalyst. The autoclave was then filled with CO_2 from an HPLC pump (Gilson 304 fitted with a cooled pump head) to a total pressure of 200 bar. The reaction solution was left for 1 h to allow the ionic liquid to absorb $scCO_2$. 1-Dodecene (2 cm^3, 9.01 mmol) was injected into the autoclave by an HPLC pump and the reaction solution was stirred at temperature and pressure for 1 h. The autoclave was then cooled to ca. −40 °C and the CO_2 was slowly vented over a period of approximately 30 min. The ionic liquid solution was extracted with hexane (3 × 15 cm^3). The hexane extract was analyzed by GC.

3. Batch Reactions of 1-Octene: Gas Uptake Measurements. [$Rh(acac)(CO)_2$] (46.8 mg, 0.18 mmol) was weighed into an autoclave (30 cm^3) fitted with a magnetically driven stirrer, pressure transducer, and thermocouple. The autoclave was purged with CO/H_2 and then charged with a solution of [PrMIM][TPPMS] **(4)** (1.31 g, 2.81 mmol) in the ionic liquid (12 cm^3), again under a CO/H_2 purge. The autoclave was pressurized with CO/H_2 (1:1, 40 bar) and heated to 100 °C with rapid stirring. The catalyst solution was stirred for 1 h at 1100 rpm, to allow for the formation of active catalyst, and then pressurized with CO_2 using an air operated liquid pump to a pressure of 200 bar. The system was left for a further 1 h to allow for gas uptake by the ionic liquid, during which the pressure was maintained at 200 bar by further additions of CO_2. Following equilibration, 1-octene (2 cm^3, 12.7 mmol) was injected directly into the ionic liquid solution through a liquid feed dip-tube using an HPLC pump. The pressure in the system was measured sequentially over a period of 1 h. We note that rate constants cannot be determined from the gas uptake curves because the measurements were not made at constant pressure.

4. Semi-continuous Reactions of 1-Nonene. The autoclave was charged with [$Rh_2(OAc)_4$] (10.3 mg, 0.047 mmol Rh), [BMIM]-[TPPMS] **(5)** (0.33 g, 0.70 mmol), 1-nonene (2 cm^3, 11.57 mmol) and the ionic liquid (4 cm^3). The solution was purged with CO/H_2 prior to pressurization with CO/H_2 (1:1, 40 bar). Carbon dioxide was then delivered into the autoclave from an HPLC pump (fitted with a refrigerated pump head) and the system heated rapidly to 100 °C with stirring to give a total system pressure of 185 bar. After 1 h, the products and any unreacted substrate were extracted from the autoclave by a continuous stream of CO_2 at the reaction temperature and pressure. The CO_2 was delivered to the inlet port of the autoclave by the HPLC pump and was decompressed into a second autoclave held at ca. −40 °C. The gas stream from the second autoclave was then passed through ethanol in a Dreschel bottle to trap any volatiles. Following a 2 h extraction, the reaction autoclave was cooled, vented to atmospheric pressure, recharged with fresh substrate and the process repeated. Meanwhile, the second autoclave was allowed to warm to room temperature and both the trapped liquid fraction and the ethanol were analyzed by GC. The samples were analyzed for rhodium by atomic absorption spectroscopy and found to be below the detection limit (0.5 ppm—equivalent to 0.003% of the rhodium loaded). In fractions 9 and

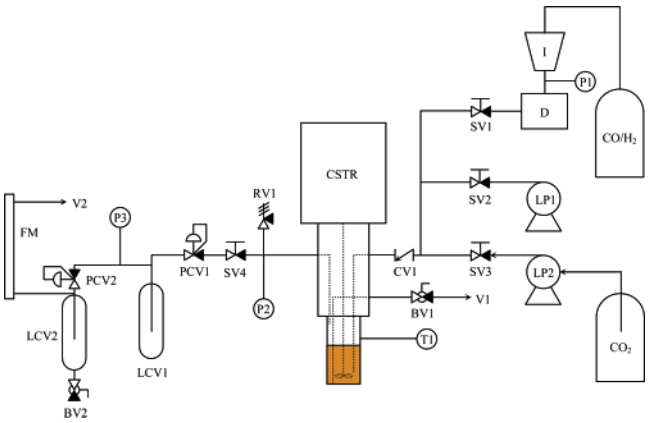

Figure 1. Reactor for continuous flow hydroformylation. **CSTR** Continuously stirred tank reactor, **CV** Check valve, **D** Dosimeter, **FM** Flow meter, **I** Intensifier, **LCV** Liquid collection vessel, **LP** Liquid pump, **P** Pressure transducer, **PCV** Pressure control valve, **RV** Relief valve, **T** Thermocouple, **SV** Shut-off valve, **V** Vent.

onward, the absorbance was approximately double that in the earlier fractions (except fraction 6, which was higher), but still below the reliable quantitative detection limit.

Similar reactions were carried out but using $P(OPh)_3$ in place of [BMIM][TPPMS]. After the fourth cycle, the reactor was opened and the ionic liquid phase analyzed by ^{31}P NMR spectroscopy. In addition to the resonance from $[PF_6]^-$ ($\delta = -157$, septet, $J_{PF} = 713$ Hz), major resonances were observed at $\delta = -17$ (t, $J_{PF} = 960$ Hz ($O_2PF_2^-$)[34]), 109 (t, $J_{PF} = 1329$ Hz) 111 (t, $J_{PF} = 1290$ Hz) and 120 (d, $J_{PF} = 1268$ Hz) ppm. We assign these last three resonances to compounds of the form $P(OPh)_nF_{3-n}$ ($n = 1$ or 2) and/or their oxides.

C. Continuous Flow Reactions (Generic Description). All continuous flow reactions were performed in the system shown schematically in Figure 1. The continuous flow system comprised a continuously stirred tank reactor (CSTR) (Hastelloy, 30 cm^3) fitted with a thermocouple (T1), pressure transducer (P2), two gas/liquid feed dip-tubes and an outlet port.

Carbon dioxide was delivered into the system to a constant pressure using an air driven liquid pump (LP2). Liquid substrates were delivered at a constant rate through an HPLC pump (LP1) and CO/H_2 was delivered through an air driven intensifier (I) coupled to a rheodyne injection unit fitted with a pneumatic actuator (D). The liquid/gas substrates and CO_2 were passed through a check valve and into the CSTR through one of the dip-tubes and into the ionic liquid solution. The gas stream leaving the CSTR was then decompressed from operating pressure to 3−10 bar (PCV1) into a vessel (LCV1) where the majority of liquid fractions were collected. The gas stream was decompressed further to atmospheric pressure (PCV2) into a second collection vessel (LCV2) after which the gas stream was passed through a flow meter.

In a typical experiment, a solution of $[Rh(acac)(CO)_2]$ (46.5 mg, 0.180 mmol) and [PrMIM][TPPMS] **(4)** (1.31 g, 2.808 mmol,) dissolved in the ionic liquid (12 cm^3) was injected into the reactor through the decompression port of the CSTR under a N_2 purge. The system was then sealed and purged with CO/H_2 (1:1) for several minutes prior to pressurization with CO/H_2 (40 bar). The system was heated with rapid stirring (1100 rpm) to 100 °C for ca. 1 h to allow for catalyst preformation. Carbon dioxide (grade N5.5, BOC) was then slowly added to the system to a pressure of 200 bar and the gas mixture was allowed to expand into the decompression stage of the system as far as the first expansion valve (PCV1). The gas expansion valves (PCV 1 & 2) were adjusted to give a fixed total gas flow through the system, as measured by a flow meter (FM) and a pressure of 4−5 bar at the inlet of the 2nd expansion valve. Synthesis gas (1:1) was then delivered into the system at a predetermined rate. With the temperature of the first expansion valve being maintained at room temperature, the liquid substrate was introduced into the system at a fixed rate by a Gilson 305 HPLC pump (LP1). The system was run continuously with the product stream being sampled and analyzed during the period of substrate injection. Mass balance was checked by weighing the collection vessels before and after the collection of each fraction. Turnover frequencies, for a given set of reactor conditions, were determined from linear regression of turnover number (TON, defined as moles of product (mol rhodium)$^{-1}$) versus time plots with a minimum of 5 data points after equilibration had been reached (2−8 h depending on reactor conditions). The point of equilibration was taken as $t = 0$. Recovered liquid fractions were analyzed by ICPMS and GC. At the end of an experiment the ionic solution was vented under pressure through V1 and analyzed by ^{31}P NMR spectroscopy.

Table 1. Hydroformylation of Hex-1-ene Catalyzed by $[Rh_2(OAc)_4]/P(OPh_3)$[a]

solvent	cosolvent	conversion/%	aldehyde selectivity/%	l:b
toluene		>99	83.9	2.5
$[BMIM]PF_6$		>99	15.7[b]	2.4
$[BMIM]PF_6$	$scCO_2$[c]	40	83.5	6.1

[a] $[Rh_2(OAc)_4]$ (10 mg, 4.5×10^{-5} mol), $P(OPh_3)$ (0.2 g, 6.7×10^{-3} mol), 1-hexene (2 cm^3, 1.8×10^2 mol), 4 cm^3 of solvent, 70 bar CO/H_2, 100 °C, 1 h. [b] The majority of the product is condensed aldehydes. [c] Total pressure = 230 bar.

D. X-ray Crystallographic Structure Determination for [PrMIM][TPPMS]. $C_{25}H_{27}N_2O_3PS$, colorless prism, 0.19 × 0.1 × 0.1 mm, monoclinic, space group $P2_1/c$, $Z = 4$, $a = 18.0248(6)$, $b = 9.6419(1)$, $c = 14.8847(5)$ Å, $\beta = 109.292(2)°$, $V = 2441(1)$ Å^3, ρ_{calcd} 1.269 Mgm^{-3}, $2\theta_{max} = 46.46°$, graphite monochromated $Mo_{K\alpha}$ radiation ($\lambda = 0.710\ 73$ Å), $\mu(Mo_{K\alpha}) = 0.227$ mm^{-1}, $T = 293$ K. Data were measured on a Bruker SMART CCD, and Lorentzian polarization and absorption (SADABS, max./min. transmission 1.0000/0.845 457) corrections were performed. Of 10 157 measured data, 3459 were unique and 2590 observed [$I > 2\sigma(I)$]. The structure was solved by direct methods. The non-hydrogen atoms were refined anisotropically, the hydrogen atoms were idealized and refined isotropically using a riding model. Structural refinements were performed with the full-matrix least-squares method on F^2 for all data (G M Sheldrick, SHELXTL Version 5.10, Bruker AXS, Madison WI, 1997) to give conventional $R_1 = 0.0433$ and $wR_2 = 0.1036$ for 290 parameters with a residual electron extremes of 0.248 and −0.163 eÅ^{-3}. All non-hydrogen atoms were refined anisotropically. Hydrogen atoms were constrained to chemically reasonable positions.

Results and Discussion

A. Batch and Semi-continuous Reactions. Our early studies of the hydroformylation of long (>C_7) chain alkenes in SCF−IL biphasic systems involved rhodium complexes of triaryl phosphite ligands. Table 1 shows results obtained from the hydroformylation of 1-hexene in the ionic liquid 1-butyl-3-methylimidazolium hexafluorophosphate ($[BMIM]PF_6$) using triphenyl phosphite as the rhodium based ligand. In the absence of $scCO_2$, the rate of alkene consumption was high but the selectivity to the desired aldehyde product was low on account of the formation of large amounts of aldol condensation products. Carrying out the same reaction in the presence of $scCO_2$ reduced the reaction rate but increased both the selectivity to the desired product aldehydes and the l:b ratio. Similar linear selectivities have previously been observed using $Rh/P(OPh)_3$ in $scCO_2$ without an ionic liquid.[19] It appears that the main role of the $scCO_2$ in this case is to reduce the residence time of the

(34) Smith, G.; Cole-Hamilton, D. J.; Gregory, A. C.; Gooden, N. G. *Polyhedron* **1982**, *1*, 97−103.

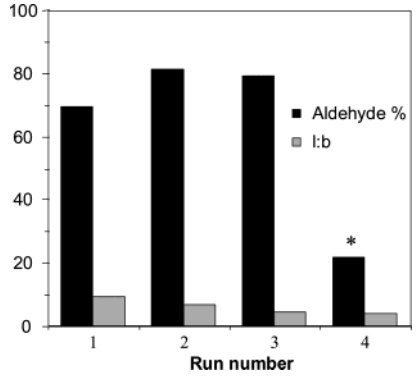

Figure 2. Repeated use of a catalyst derived from $[Rh(CO)_2(acac)]$ and excess $P(OPh)_3$ for the hydroformylation of 1-nonene in $[BMIM]PF_6$/ $scCO_2$. For detailed conditions, see the Experimental Section.

product aldehyde in the catalyst solution and protect it from further reaction.

We carried out similar reactions of 1-hexene or 1-nonene in the biphasic system, extracting the products from the reactor with $scCO_2$, which was decompressed into a second autoclave held at low temperature. Following the CO_2 extraction, the reactor was cooled, depressurized, and recharged with fresh substrate, CO, H_2, and CO_2. This semi-continuous operation could be repeated for 2−3 runs with the same batch of catalyst. However, a gradual decrease in the selectivity was observed and reactivity dropped severely after the third cycle (see Figure 2). ^{31}P NMR analysis of the ionic liquid phase after the 4th cycle showed that it contained a significant concentration of $O_2PF_2^-$ and fluorinated phosphorus compounds of the form $P(OR)_nF_{3-n}$ (where $n = 1-2$) and/or their oxides. These products arise from the reaction of the PF_6^- anion with water, presumably released during the aldol condensation reactions, followed by attack of released HF on the phosphite ligands. Such degradation of PF_6^- has been known for many years.[34] The lower rate and selectivity in the 4th cycle, despite the addition of excess $P(OPh)_3$, suggests that the fluorinated phosphorus compounds are better ligands for rhodium than the phosphite itself. Attack of HF on the rhodium center may also occur, but we did not directly observe this.

We therefore turned our attention to sulfonated triphenylphosphine ligands, which had originally been designed for reactions in aqueous biphasic systems[3,8] but had also been used with moderate success for the hydroformylation of alkenes in ionic liquids.[35] Using sodium salts of the sulfonated triphenylphosphine ligands, resulted in overall yields that were rather low, and inspection of the reaction solutions through a sapphire window situated in the bottom of the autoclave indicated that the catalysts were only partially soluble. Exchanging sodium for the BMIM cation, however, gave catalysts which showed high reactivity. A catalyst synthesized in situ from [BMIM]-[TPPMS] (which has also been reported to be very suitable for reactions using supported ionic liquids[36]) was reused several times for the hydroformylation of 1-octene in the semi-continuous system described above. The results are shown in Figure 3. With repetitive use, the rate of reaction varies in an unusual manner while the l:b ratio drops monotonically (from 3.6 to 2.6) over the course of the experiments. After the catalyst

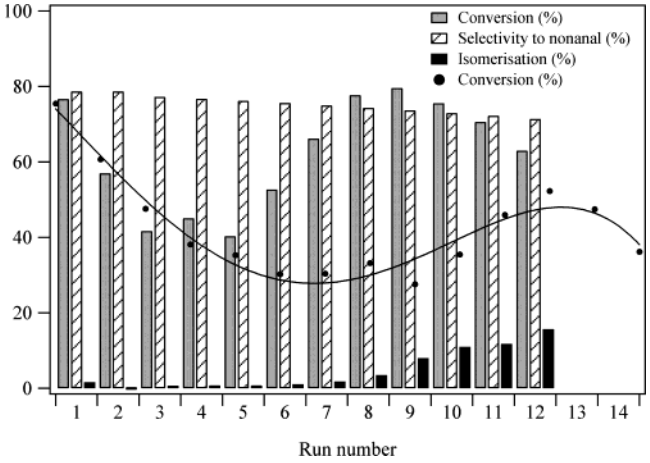

Figure 3. Semi-continuous hydroformylation of 1-nonene catalyzed by Rh/$[Ph_2PC_6H_4SO_3]$[BMIM] in $[BMIM]PF_6$ (bar chart) or Rh/$[Ph_2PC_6H_4SO_3]$-[BDMIM] in $[BDMIM]PF_6$ (line). Rhodium is undetected up to reaction 9 (<0.03% of Rh loaded), but increases thereafter.

has been reused several times, rhodium starts to be observed in the recovered product and there is a corresponding increase in the levels of alkene isomerization. This behavior is reproducible and occurs whether the ionic liquid is $[BMIM]PF_6$ or $[BDMIM]PF_6$ (**3**), in which the hydrogen atom at the 2-position of the imidazolium cation is replaced by methyl.

After 12 runs, the ionic liquid phase was analyzed by ^{31}P NMR spectroscopy and it was found that all of the phosphine had been oxidized to phosphine oxide. Assuming that the phosphine is being oxidized over the course of the reaction, which effectively reduces the phosphine concentration, we offer the following explanation of the catalytic results. Excess tertiary phosphine is known to inhibit hydroformylation reactions, whereas monophosphine complexes are less active than their bisphosphine analogues.[1,2] The drop in rate over the first 5 runs presumably arises because monophosphine species become significant and increase in concentration. The rate then falls until there is a significant concentration of unmodified rhodium (i.e., $[RhH(CO)_4]$ from $[Rh_4(CO)_{12}]$). This unmodified rhodium complex has been shown to be highly active for hydroformylation in $scCO_2$,[37] is much less selective toward the linear aldehyde than phosphine modified catalysts and is a good alkene isomerization catalyst. Furthermore, the higher solubility of $[Rh_4(CO)_{12}]$ in $scCO_2$ accounts for the slightly enhanced rhodium leaching which occurs from the ninth experiment onward. The drop in rate in the later cycles may arise because the rhodium concentration is decreasing as it is removed from the reactor in the $scCO_2$. The detrimental oxidation of the phosphine presumably arose because of the inadvertent admission of air into the system during the very many handling steps required for the semi-continuous process. A related effect of oxygen, although much less marked, is also observed in the continuous flow experiments (see below).

B. Continuous Flow Reactions. 1. Initial Reactions. To overcome the problem of phosphine oxidation and to make the process continuous, we constructed the apparatus shown schematically in Figure 1. The continuously stirred tank reactor (CSTR) contains the ionic catalyst dissolved in the ionic liquid, while the substrate, permanent gases and CO_2 are all metered separately and continuously into the reactor (see the Experimental Section for a detailed description). The $scCO_2$ containing

(35) Chauvin, Y.; Mussmann, L.; Olivier, H. *Angew. Chem., Int. Ed. Engl.* **1996**, *34*, 2698−2700.

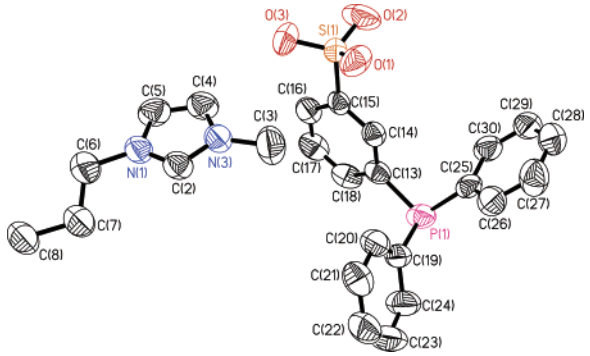

Figure 4. Structure of [PrMIM][TPPMS] in the crystal (50% thermal ellipsoids, hydrogen atoms omitted for clarity). Selected bond lengths (Å) and angles (°). N(1)−C(2) 1.314(3), N(1)−C(5) 1.368(4), N(1)−C(6) 1.482(4), C(2)−N(3) 1.325(3), N(3)−C(4) 1.361(4), N(3)−C(3) 1.468(4), C(4)−C(5) 1.339(4), P(1)−C(13) 1.832(3), P(1)−C(25) 1.834(3), P(1)−C(19) 1.842(3), C(15)−S(1) 1.781(3), S(1)−O(1), 1.445(2) S(1)−O(2) 1.427(2), S(1)−O(3) 1.441(2); C(2)−N(1)−C(6) 126.3(3), C(5)−N(1)−C(6) 125.0(3), N(1)−C(2)−N(3) 108.8(2), C(2)−N(3)−C(4) 108.2(2), C(2)−N(3)−C(3) 125.4(3), C(4)−N(3)−C(3) 126.3(3), C(5)−C(4)−N(3) 107.5(3), C(4)−C(5)−N(1) 106.9(3), C(13)−P(1)−C(25) 101.47(13), C(13)−P(1)−C(19) 102.31(12), C(25)−P(1)−C(19) 102.42(14), O(2)−S(1)−O(3) 113.28(15), O(2)−S(1)−O(1) 113.87(17), O(3)−S(1)−O(1) 111.70(13), O(2)−S(1)−C(15) 105.74(13), O(3)−S(1)−C(15) 106.12(12),O(1)−S(1)−C(15) 105.30(12).

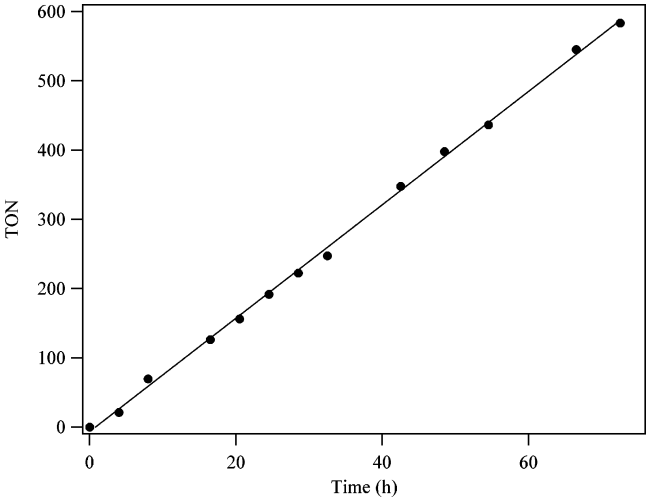

Figure 5. Continuous flow hydroformylation of 1-octene catalyzed by $Rh/[PrMIM]_2[PhP(3\text{-}C_6H_4SO_3)_2]$, over 3 days. l:b = 3.8 throughout. Conditions as in experimental with a CO flow rate of 1.85 mmol min^{-1} ($CO:H_2$ = 1:1) a 1-octene flow rate of 0.2 mmol min^{-1} and a CO_2 flow rate of 0.78 normal liters per minute (nL min^{-1}).

the products and any unreacted starting materials is then decompressed downstream in two stages, after which the product is collected and the $scCO_2$ vented. Initial studies in the continuous flow system were carried out using $[BMIM]PF_6$ as the ionic liquid and a catalyst derived from $[Rh_2(OAc)_4]$ and $[PrMIM]_2[PhP(3\text{-}C_6H_4SO_3)_2]$, although later studies employed [PrMIM][TPPMS] **(4)** because it is easy to crystallize and purify. The structure of **(4)** (Figure 4) reveals the expected pattern of delocalisation in the imidazolium cation with the N_2C_3 ring being perfectly planar (mean deviation 0.002 Å); the C(3) and C(6) substituents lie 0.04 and −0.08 above and below the ring plane, respectively.

The results of a typical reaction using $[PrMIM]_2[PhP(3\text{-}C_6H_4SO_3)_2]$, run continuously over 3 days, are shown in Figure 5. The linearity of the graph and the constant l:b ratio of 3.8 confirm that the catalyst is stable under the reaction conditions for at least 3 days without any visible sign of phosphine oxidation.

These initial results demonstrated that continuous flow reactions are possible using homogeneous catalysts, even with substrates of relatively low volatility. However, conversions (ca. 10%) and rates (5−10 catalyst turnovers h^{-1}, cf. 500−700 h^{-1} in the commercial hydroformylation of propene catalyzed by rhodium) were very low and selectivity to the desired linear product was moderate (l:b ratios of 3.8 cf. 6 for the commercial process). Problems were also encountered upon decompression of the CSTR which resulted in extensive foaming of the ionic liquid phase. This foaming caused catalyst to be deposited throughout the system leading to unacceptably long down times for cleaning. There was also evidence for some entrainment of the catalyst solution in the early parts of reactions so that rhodium loss from the reactor occurred in the first fractions collected. Finally, the mass balance for the reactions was very poor, with only about 20% of the mass of substrate injected being accounted for in the liquid fractions collected downstream. The material lost was assumed to be substrate alkene, so that the turnover numbers shown in Figure 5 represent conservative values. We have since modified the CSTR by installing a liquid sampling tube through which the catalyst solution can be removed under pressure, thereby preventing contamination of the pipework and decompression system. We have redesigned the collection system so that the bulk of the product is collected between the two decompression stages and collection efficiencies are now routinely >90% (this configuration is shown in Figure 1). We have also modified the reaction conditions to address the problem of very low rates and this is the subject of the optimization reactions discussed below. Improving the selectivity to linear aldehyde, which involves the use of different ligands, will be the subject of a separate report.[38]

C. Optimization Reactions. 1. Alternative Ionic Liquids. Although $[BMIM]PF_6$ has been the most studied of the ionic liquids for hydroformylation and other catalytic reactions,[39−43] the solubility of alkenes within it is not very high. The partitioning of an alkene toward the gaseous phase in the $[BMIM]PF_6/scCO_2$ system results in rates in the continuous flow process that are determined largely by mass transport limitations. The low catalyst turnovers initially observed are then hardly surprising because the reaction relies on the dissolution of a lipophilic substrate in an ionic solution. This mass transport limitation is analogous to that found in the aqueous-biphasic process described earlier, which as a consequence is limited to alkenes with <6 carbon atoms. In an attempt to overcome mass transport limitations, we have focused on the design of ionic liquids that are more capable of solubilizing nonpolar substrates. Wasserscheid has reported[44] that the solubility of alkenes in

(36) Mehnert, C. P.; Cook, R. A.; Dispenziere, N. C.; Afeworki, M. *J. Am. Chem. Soc.* **2002**, *124*, 12 932−12 933.
(37) Koch, D.; Leitner, W. *J. Am. Chem. Soc.* **1998**, *120*, 13 398−13 404.
(38) Kunene, T. E.; Webb, P. B.; Cole-Hamilton, D. J. **2003**, Manuscript in preparation.
(39) Dupont, J.; Silva, S. M.; de Souza, R. F. *Catal. Lett.* **2001**, *77*, 131−133.
(40) Favre, F.; Olivier-Bourbigou, H.; Commereuc, D.; Saussine, L. *Chem. Commun.* **2001**, 1360−1361.
(41) Brauer, D. J.; Kottsieper, K. W.; Liek, C.; Stelzer, O.; Waffenschmidt, H.; Wasserscheid, P. *J. Organomet. Chem.* **2001**, *630*, 177−184.
(42) Brasse, C. C.; Englert, U.; Salzer, A.; Waffenschmidt, H.; Wasserscheid, P. *Organometallics* **2000**, *19*, 3818−3823.
(43) Wasserscheid, P.; Waffenschmidt, H.; Machnitzki, P.; Kottsieper, K. W.; Stelzer, O. *Chem. Commun.* **2001**, 451−452.
(44) Wasserscheid, P.; Keim, W. *Angew. Chem., Int. Ed.* **2000**, *39*, 3773−3789.

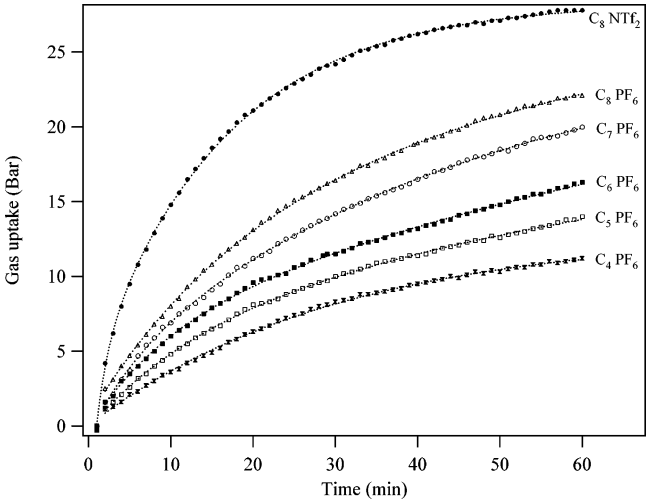

Figure 6. Effect of anion and alkyl group in the 1-position of 1-alkyl-3-methylimidazolium salts on reaction rate for the hydroformylation of 1-octene in a batch reactor using Rh/[PrMIM][$Ph_2P(3\text{-}C_6H_4SO_3)$] and $scCO_2$. Conditions are given in the the Experimental Section.

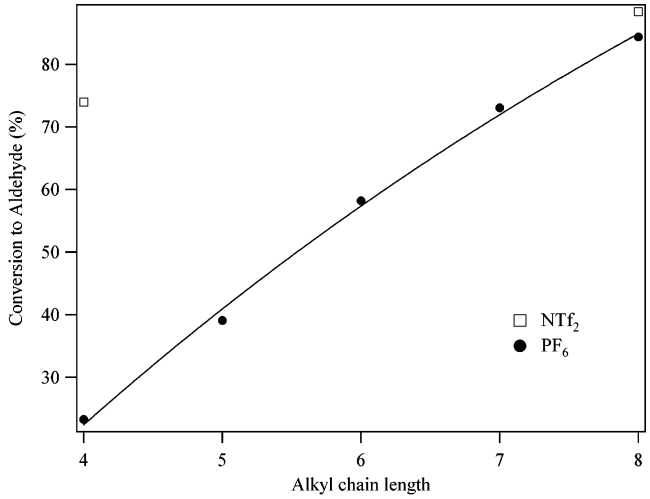

Figure 7. Effect of anion and alkyl group in the 1-position of 1-alkyl-3-methylimidazolium salts on reaction rate (conversion in 1 h) for the hydroformylation of 1-dodecene in a batch reactor using Rh/[PrMIM]-[$Ph_2P(3\text{-}C_6H_4SO_3)$] and $scCO_2$.

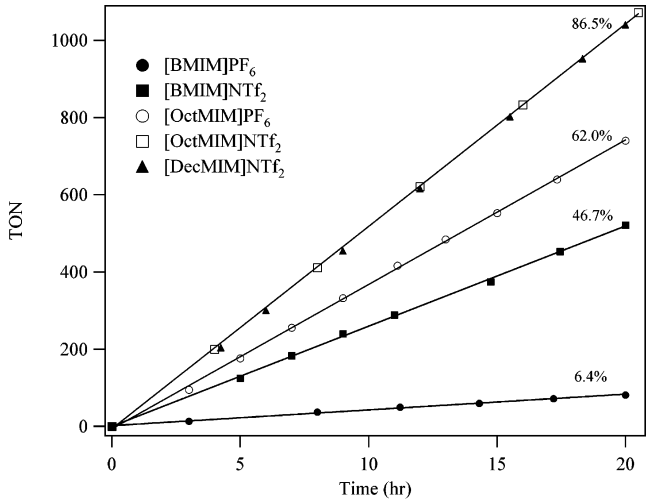

Figure 8. Hydroformylation of 1-dodecene catalyzed by Rh/[PrMIM]-[$Ph_2P(3\text{-}C_6H_4SO_3)$] in a variety of ionic liquids. The numbers are conversions of 1-dodecene in the isolated fractions. Conditions as given in the Experimental Section using a CO flow rate of 1.85 mmol min^{-1} ($CO:H_2$ = 1:1), a 1-dodecene flow rate of 0.19 mmol min^{-1} and a CO_2 flow rate of 0.78 nL min^{-1}. Rhodium and phosphine concentrations are constant throughout the continuous flow experiments at 15 mM and 234 mM, respectively.

ionic liquids can be increased by replacing the butyl group of [BMIM]PF_6 with longer alkyl chains and more recent studies have shown related effects.[29] We therefore carried out reactions in a range of ionic liquids where the alkyl chain of the imidazole was varied from butyl to decyl. The different ionic liquids were initially screened by monitoring the rate of gas uptake in batch reactions using 1-octene as the substrate.

It is clear from Figure 6 that the rate increases dramatically as the alkyl chain length is increased to octyl. Further rate enhancements are observed if the PF_6 anion is replaced by the bis(trifluoromethanesulfonyl)amide (NTf_2) anion. Sulfonyl amide salts have the added advantage that they are not sensitive to moisture and also appear to be less prone to foaming. We believe that this foaming, which becomes increasingly worse for the longer alkyl chain imidazoles, arises because these ionic liquids behave like surfactants. Replacing the PF_6 anion by one of a lower charge density appears to suppress the surfactant-like behavior. Although changes in viscosity and better transport of CO and H_2 into the ionic liquid may in part be responsible for the increased rates, we believe that increased solubility of the alkene is the dominating factor. Figure 7 shows that the increased rate is also observed for the imidazolium salts with longer alkyl chains when 1-dodecene is used as the substrate, while Figure 8 shows the result of using different ionic liquids for the hydroformylation of 1-dodecene in the continuous flow system. Once again, dramatic increases in rate are observed and the conversion can be higher than 80%. We note that 100% conversion in a continuous flow reaction is unlikely when only one reactor is used because some substrate will travel through the reactor without contacting the catalyst. Improvements could be obtained by using cascade reactors. Since [1-octyl-3-methylimidazolium]NTf_2 ([OctMIM]NTf_2) proved to be the most effective ionic liquid of those screened, it was used in all subsequent studies. We note that increasing the alkyl chain length of imiazolium based ionic liquids is believed to lead to greater toxicity.[45]

D. Effect of Substrate Flow Rate. Initial studies were carried out at low substrate flow rates, assuming that the longer the residence time of the substrate, the higher would be the percentage conversion to products. We believe that at these low flow rates, all of the substrate that contacts the catalyst is converted into products, so that improved productivity at higher flow rates may be obtained. The productivity, as indicated by catalyst turnover frequency (TOF) in Figure 9, does indeed increase with an increase in substrate flow rate, although the percentage of aldehyde in the recovered solution decreases. The increase in TOF with flow rate is not linear, but tends to a maximum value, where the reaction kinetics are the dominant controlling factor. The saturation value appears to depend on other reaction parameters such as the concentration of the ligand (Figure 9, broken line) which will be discussed in a later section. Importantly, the turnover frequency at these higher substrate flow rates can be > 500 $h^{-1}$and represents a 50−100 fold increase over the rates we initially reported.

Figure 10 illustrates results obtained for 1-octene, 1-dodecene and styrene obtained under otherwise identical conditions. We observe little dependence of the rate upon the nature of the

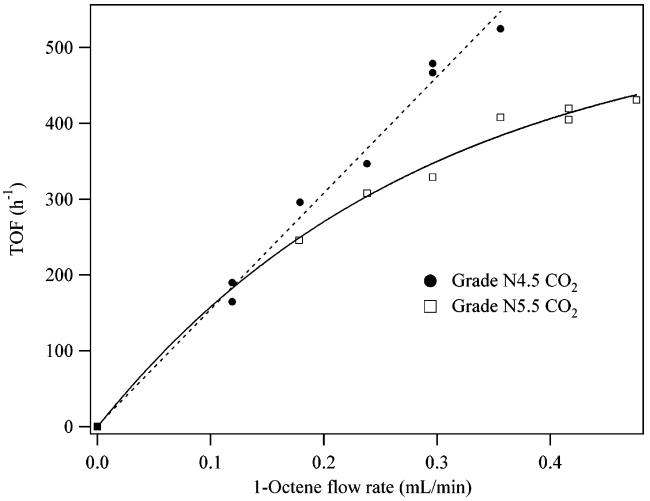

Figure 9. Continuous flow hydroformylation of 1-octene catalyzed by Rh/[PrMIM][$Ph_2P(3\text{-}C_6H_4SO_3)$] in the [OctMIM]$NTf_2/CO_2$ biphasic system • using technical grade (99.995%) CO_2 at 200 bar, 100 °C and a CO flow rate of 3.77 mmol min^{-1} ($CO:H_2$ = 1:1); and □ using high purity CO_2 (99.9995%) under otherwise identical conditions. The CO_2 flow rate was fixed at 1.00 nL min^{-1}. Note: Separate catalyst solutions were used with each grade of CO_2 with the data being collected in the order of increasing octene flow rate.

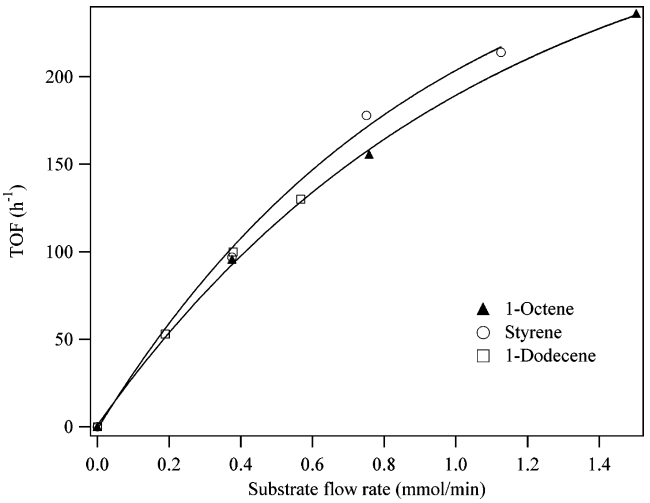

Figure 10. Continuous flow hydroformylation of 1-octene, 1-dodecene, and styrene catalyzed by Rh/[PrMIM][$Ph_2P(3\text{-}C_6H_4SO_3)$] in the [OctMIM]-$NTf_2/CO_2$ biphasic system at 200 bar, 100 °C, and a CO flow rate of 1.85 mmol min^{-1} ($CO:H_2$ = 1:1). The CO_2 flow rate was fixed at 0.65 nL min^{-1}.

substrate at these low flow rates, providing further evidence that all substrate which contacts the catalyst reacts under these conditions.

E. Effect of Temperature. The supercritical fluid−ionic liquid (SCF−IL) biphasic system relies on the partition of product between gas and liquid phases for separation purposes. However, the substrate also partitions between the two phases as demonstrated by the observation that complete conversion of the substrate is never achieved with reasonable flow rates. There is therefore scope for increasing the reaction rate if the fraction of substrate dissolved in the ionic liquid can be increased. A shift in the equilibrium partitioning of the substrate can be effected by modification of the ionic liquid phase as described above but can also be achieved by tuning the solvent properties of the gaseous phase. A substance above its critical temperature cannot be liquefied by compression alone enabling a range of densities to be obtained (from gaslike to liquidlike

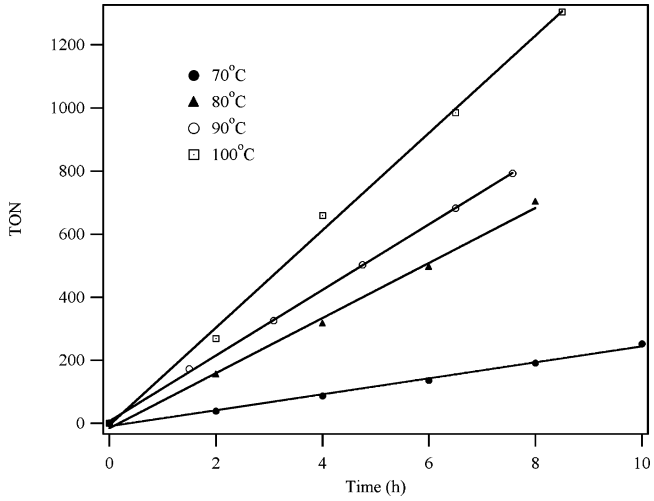

Figure 11. Continuous hydroformylation of 1-octene catalyzed by Rh/[PrMIM][$Ph_2P(3\text{-}C_6H_4SO_3)$] in the [OctMIM]$NTf_2/CO_2$ biphasic system as a function of temperature.

values) without the emergence of a phase boundary. This ability to continuously tune the density of a SCF gives rise, in part, to its tunable solvent properties. Unlike normal liquid solvents, which rely on chemical interaction for the process of dissolution, SCF's also possess an additional state effect giving rise to complex solvent behavior as a function of both temperature and pressure. The addition of a permanent gas to a SCF will also affect its solvent properties. The additional gas causes the SCF to expand so that its density and solvating capacity are reduced. It should therefore be possible to operate the continuous flow process under conditions which will partition the substrate more favorably toward the ionic liquid phase. In principle, this can be achieved by reducing the temperature or pressure of the system or by control over the relative concentration of CO/H_2.

Figure 11 shows the data obtained for the continuous hydroformylation of 1-octene as a function of temperature. Although there are minor differences in the compositions of the gaseous phase in each case, it can be seen clearly that the rate drops dramatically with decreasing temperature despite the fact that in principle the distribution of the solute should shift toward the ionic liquid phase as its vapor pressure is reduced. What we actually observe in this case is normal Arrhenius behavior because, under the higher substrate flow conditions of these measurements, where the reaction kinetics dominate, what we gain from the increased concentration of the substrate in the ionic liquid is more than lost by the slower reaction kinetics at the lower temperature. It is probable that increases in total conversion and therefore apparent reaction rate could be observed at lower temperatures under low flow rate conditions, but we have not examined this.

F. Effect of Gas Composition. The dependence of hydroformylation reaction rates on CO and H_2 partial pressure is complex. Usually, the reactions show a zero or positive order in hydrogen and a negative order in carbon monoxide;[1] although a positive order in both has been observed in $scCO_2$ when using triethylphosphine as the ligand.[20] When the partial pressures of both CO and H_2 are changed together, thus keeping the $CO:H_2$ ratio constant, the behavior depends on the actual orders in both cases. Figure 12 demonstrates the effect of the concentration of CO/H_2 at levels which are high enough to suppress catalyst leaching (see below). Here, we observe an exponential increase

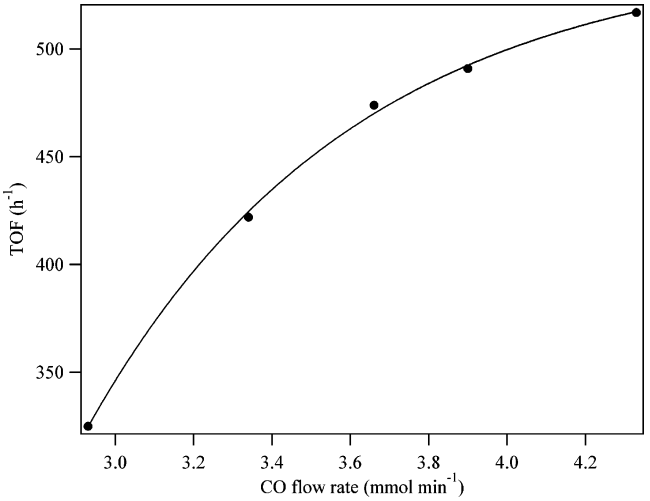

Figure 12. Effect of CO/H_2 (1:1) flow rate (equivalent to partial pressure) on the rate of hydroformylation of 1-octene (2.65 mmol min^{-1}) catalyzed by Rh/[PrMIM][TPPMS] (**4**) in the [OctMIM]NTf_2/CO_2 biphasic system. The CO_2 flow rate is kept constant throughout at 1.00 nL min^{-1}. See the Experimental Section for details of conditions.

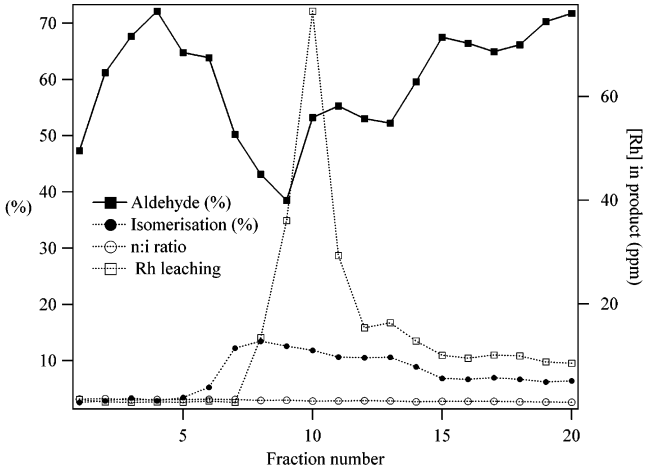

Figure 13. Effect of changing the partial pressure of CO/H_2 during the continuous hydroformylation of 1-octene (0.76 mmol min^{-1}) using a catalyst formed in situ from [Rh(CO)(acac)$_2$] (49.2 mg, 0.19 mmol) and [PrMIM]-[$Ph_2P(3\text{-}C_6H_4SO_3)$] (1.31 g, 2.808 mmol) in [OctMIM]NTf_2 (12 cm^3) and CO_2 (total pressure = 200 bar). The initial CO flow rate was 1.86 mmol min^{-1} this was altered to 0.8 mmol min^{-1} at fraction 6, 1.12 mmol min^{-1} at fraction 10, 1.86 mmol min^{-1} at fraction 14 and 2.66 at fraction 18. The CO_2 flow rate is constant throughout the measurements at 1.00 nL min^{-1}. Further details can be found in the Experimental Section.

in rate with an increasing concentration of reactant gas up to a saturation limit.

At first sight, this appears to indicate an overall positive order in CO/H_2. However, we interpret the increased reaction rate at higher CO/H_2 partial pressures as a shift in the equilibrium partitioning of substrate toward the ionic liquid phase. The shift in substrate distribution arises due to a change in the solvent properties of the supercritical phase caused by the permanent gases, as previously discussed. This increased substrate concentration is then responsible for an increase in reaction rate. We believe that it is this effect that dominates the dependence of the reaction rate on the flow rate (partial pressure) of CO/H_2 and not an overall positive order in reactant gas.

Whereas high partial pressures of CO/H_2 improve productivity there is an upper limit to the concentration of reactant gas that can be employed. Too high a partial pressure of CO and H_2 will eventually reduce the solvating properties of the gaseous phase to such an extent that it will have a detrimental effect on the solubility of both substrate and product in the supercritical phase. Under such conditions, the product will not be removed from the reactor at a rate equivalent to the substrate feed and mass balance will not be achieved. The product will then accumulate in the reactor until it is full and is forced out together with the catalyst and ionic liquid. Mass balance measurements show that this situation has been reached at the highest flow rate presented in Figure 12.

We have also carried out these studies with much lower partial pressures of CO/H_2. Figure 13 shows the result of drastically reducing the CO/H_2 partial pressure and then returning it back to and beyond its original value. The effect of the composition of the gaseous phase appears 2-fold. First, we again observe a decrease in rate when the partial pressure of CO and H_2 is reduced and the extent of isomerization increases markedly, as expected for the lower CO partial pressure. Second, there is a significant increase in the extent of rhodium leaching into the isolated product when the CO/H_2 partial pressure is reduced. These effects can be reversed by increasing the partial pressure of CO/H_2 back toward its original value. The failure of the system to return exactly to its original state is masked in this case by partial oxidation of the ligand (see below). The marked increase in rhodium leaching on decreasing the concentration of CO/H_2 can also be attributed to a corresponding change in the solvent properties of the gaseous phase. Again, dissolution of the catalyst in the mobile phase can be suppressed by increasing the partial pressure of the permanent gases and thus reducing the solvating power of the supercritical phase.

In summary, an increase in the partial pressure of CO/H_2 increases the reaction productivity and decreases the catalyst leaching because both the substrate and catalyst partition more into the ionic liquid. However, there is an upper limit to the partial pressure of CO/H_2, which can be used successfully. This is determined by the ability of the supercritical phase to remove the reaction product at a rate equivalent to that of the substrate feed. The equilibrium distribution of liquid substrate may also be affected by reducing the total system pressure with the advantage that lower concentrations of reactant gas may be used.

G. Long-Term Stability of the Catalyst. One sample of catalyst solution was used for a variety of different reactions over a period of 80 h. The solution was kept at the reaction temperature and pressure throughout this period although the substrate was only flowing off and on for about 40 of the 80 h. After this 80 h period, the reactor was held at temperature and pressure (product, excess CO and H_2 were still present) for 4 weeks. The substrate flow and product collection were restarted to give identical rates and product distributions to those that were obtained immediately prior to switching off the flow. After a further 8 h period, the catalyst solution was removed from the reactor and analyzed by ^{31}P NMR spectroscopy. Some of the phosphine remained intact, but a significant proportion had been converted to phosphine oxide, showing that although the catalyst and ionic liquid are stable under the reaction conditions, the phosphine is very susceptible to oxidation in the system, even though stringent attempts were made to exclude oxygen. This effect is further demonstrated in Figure 9 for two reactions carried out using 1-octene as the substrate under identical conditions, but using different sources (purities) of CO_2. The

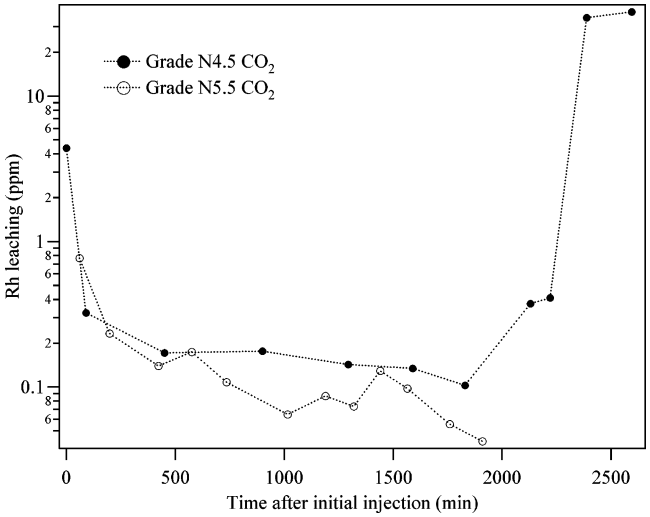

Figure 14. Rhodium concentrations in fractions collected during the hydroformylation of octene using different grades of CO_2. Conditions as in Figure 9.

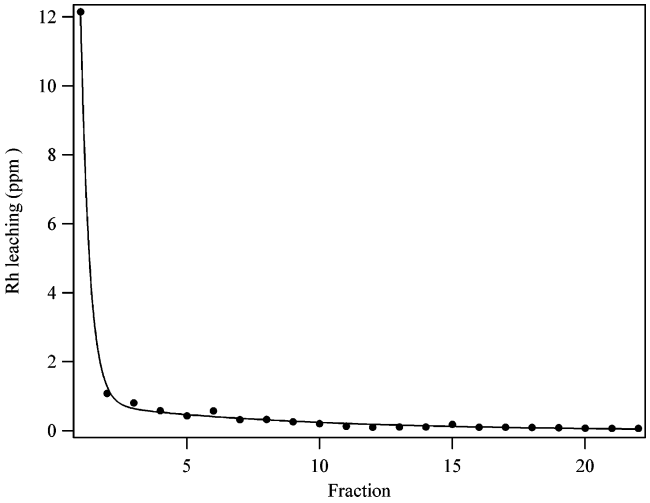

Figure 15. Rhodium loss during the hydroformylation of styrene. The steady-state value is ca. 0.1 ppm. Conditions as in Figure 10.

more highly purified CO_2 gave the results demonstrating saturation kinetics, whereas the less pure CO_2 gave a linear dependence of reaction rate on substrate flow rate. At the end of the two reactions, the ionic liquid phase was analyzed and in both cases oxidation of the phosphine had occurred. However, the extent of oxidation was much higher (>95%) for the reaction using the lower grade CO_2 than that using the higher purity (50% as determined from ^{31}P NMR integration). We interpret the linear dependence of reaction rate on substrate flow rate when using the less pure CO_2 as a composite effect. The percentage conversion does drop with an increasing substrate flow rate, but the oxidation of the ligand leads to a more active catalyst. Excess phosphine is known to reduce the reaction rate in PPh_3 promoted rhodium based hydroformylation catalysis and this has also been demonstrated to be the case for the batch system, as shown in Figure 3. Support for the suggestion that phosphine loss causes the differences between the reactions carried out under different purities of CO_2 is given by Figure 14 in which the rhodium leaching for the two reactions is compared (note the logarithmic scale). With the higher purity CO_2, the rhodium concentration in the recovered fractions was constant at <0.1 ppm for all fractions after an initial surge, whereas, when using the less pure CO_2, the concentration in the later fractions rose as high as 35 ppm. The reactions were at temperature and pressure for approximately the same time. The increased leaching suggests that the rhodium is solubilizing in the $scCO_2$ as $[Rh_4(CO)_{12}]$ because all of the phosphine has been oxidized. At these later stages, we also observe a corresponding increase in the levels of alkene isomerization which provides further evidence that the reaction is being catalyzed by unmodified rhodium.

In the run shown in Figure 9 for 1-octene using the higher purity CO_2, the reaction was on stream for 41.6 h, whereas the catalyst was at temperature and pressure for 60 h. A total of 621 cm^3 (444 g) of 1-octene was fed into the reactor during this time, and the total mass collected downstream was 446 g, although a small amount of product remained in the reactor at the end of the reaction. This represents an average mass balance of ~88% and a total production of 330 cm^3 of aldehyde from the 12 cm^3 of catalyst solution (mass balance is substrate flow dependent and is >90% at higher flow rates). GC analysis of the recovered fractions shows the presence of substrate and aldehyde products only with ca. 1.5% isomerization to internal alkenes.

H. Rhodium Leaching. One of the advantages of the SCF−IL biphasic system is the built-in separation of the product from the catalyst and the solvent. The separation of liquids from the gaseous product stream is a facile process brought about by decompression. When an SCF mixture is expanded at ambient conditions its solvating capacity is immediately lost causing precipitation of anything dissolved in it. Like any biphasic system, the trick is to control what is soluble in what. It is important that all of the catalyst remains in the ionic liquid and none is transported out of the reactor in the $scCO_2$. Although the catalyst is ionic this does not mean that it will be completely insoluble in CO_2 and indeed charge separated species have previously been shown to be CO_2 soluble.[46] The solubility of the catalyst under low partial pressures of synthesis gas was discussed previously. We have analyzed many of the product fractions using Inductively Coupled Plasma Mass Spectrometry to determine the levels of Rh leaching. Figures 13−15 show representative traces obtained from reactions using 1-octene and styrene.

The very first fractions contain significant amounts of rhodium, although this can be improved if the catalyst is preformed outside the reactor (Figure 13). In general, the value during steady-state operation is < 0.1 ppm, whereas the best results in terms of catalyst leaching were obtained under the higher CO/H_2 partial pressures of Figure 12, presumably again because the solubilizing power of the CO_2 is reduced by the higher concentration of permanent gases. The concentration of rhodium in these fractions is 0.012 ppm, which is equivalent to 1 g of rhodium in approximately 40 tons of product throughout the steady-state reaction.

A photograph of the product fractions obtained from the hydroformylation of styrene together with the solution recovered at the end of the reaction is shown in Figure 16.

(45) Jastorff, B.; Stormann, R.; Ranke, J.; Molter, K.; Stock, F.; Oberheitmann, B.; Hoffmann, W.; Hoffmann, J.; Nuchter, M.; Ondruschka, B.; Filser, J. *Green Chem.* **2003**, *5*, 136−142.
(46) Burk, M. J.; Feng, S. G.; Gross, M. F.; Tumas, W. *J. Am. Chem. Soc.* **1995**, *117*, 8277−8278.

Table 2. Comparison of Supercritical Fluid−Ionic Liquid Biphasic System with Commercial Systems[2] for the Hydroformylation of Alkenes

substrate	system	[M]/mmol dm^{-3}	[P]/mmol dm^{-3}	T/°C	p/bar	space time yield[a]/h^{-1}	rate/mol dm^{-3} h^{-1}	TOF[b]/h^{-1}	linear aldehyde/%
propene	Rh/PPh_3	2.7	286	95	18	0.19	2.1	770	89.5
propene	Rh/PPh_3	1.8	150	110	16	0.09	1.0	556	84
1-octene	Co	80		160	300	0.48	2.8	35	72
1-octene	Co/PR_3	90	270	170	60	0.31	1.8	20	87.5
1-octene	this work	15	225	100	200	1.37	8.0	517	76

[a] Space time yield is the volume of aldehyde produced per volume of catalyst solution per hour. [b] Turnover frequency (moles of product (mole of catalyst)$^{-1}$ h^{-1}.

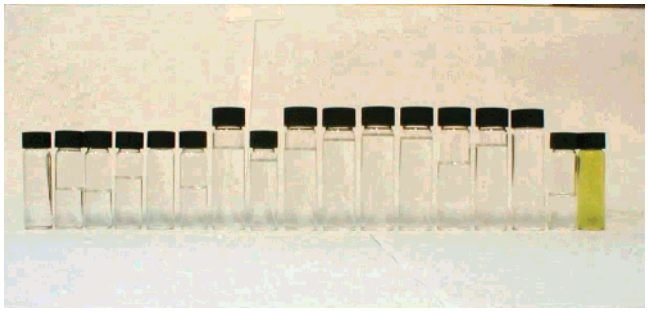

Figure 16. Solutions collected during the hydroformylation of styrene. The solution at the right-hand side was recovered from the reactor at the end of the reaction. Conditions as in Figure 10.

I. Comparison with Commercial Systems. Commercially, the hydroformylation of long chain alkenes is carried out using cobalt based catalysts, sometimes modified with tertiary phosphines.[2] The product is separated from the catalyst by a complex process involving the extraction of Co^{II} complexes into water and regeneration although some loss of Co still occurs. Rhodium catalysts have not been commercialised for this reaction despite their attractive features of milder operating conditions and higher selectivity to the desired linear aldehyde because of the problems associated with the separation of the product from the catalyst. A pilot plant using rhodium based catalysts and low pressure distillation for detergent range aldehydes is currently under construction.[47]

Table 2 presents a comparison of the results obtained for the hydroformylation of 1-octene in this study of the SCF−IL biphasic system with those obtained using cobalt based catalysts with or without added tertiary phosphine. A comparison is also given with rhodium based catalyst systems for propene hydroformylation. Cobalt catalysts are used at high concentration and require high pressures and temperatures, although these are moderated by the addition of tertiary phosphines, which also lead to the production of alcohols rather than aldehydes and the loss of some product as alkane.[2] Catalyst turnover frequencies are low, but space-time yields are high because of the high catalyst loading. The rhodium-based catalysts are much more active than their cobalt counterparts and operate under mild conditions, but with a large excess of PPh_3. The linear selectivities are also generally much higher, although it should be noted that loss of alkene by isomerization is not possible for propene. In the case of cobalt catalysts, extensive isomerization occurs, but the isomerized alkene hydroformylates predominantly to the linear aldehyde or alcohol, so that this does not represent a loss of substrate. From the results reported in this paper, it is clear that commercially acceptable rates in terms of turnover numbers and space-time yields are available and that rhodium losses are small although not yet negligible. The main problem with the system is the high pressure required, although this is no higher than that used in unmodified cobalt based systems. Further to this, the l:b ratio, which is only of the order of 3, gives a linear aldehyde selectivity of ca. 75%, whereas values >80% are desirable for commercialisation. We are addressing this problem using an alternative ligand design.[38]

(47) Harrison, G., Stockton on Tees, 2000.

Conclusions

We have demonstrated the first homogeneous catalytic system where reactions of a relatively low volatility product can be performed in a continuous flow process. This is achieved by using an ionic catalyst dissolved in an ionic liquid and using $scCO_2$ as the transport vector for the substrates and products. By careful selection of the ionic liquid, the catalyst and the reaction parameters, assisted by reactor design, we have shown that the system can be used for the hydroformylation of long chain alkenes (we have demonstrated up to 1-dodecene) at rates comparable with those found in commercial systems. Minimal catalyst leaching occurs (3.6 μg per mole product) but the linear selectivity of the process is lower than desired.

One of the appealing features of the SCF−IL process is its low potential impact on the environment. The catalyst and ionic liquid remain in the reactor at all times. Carbon dioxide is a byproduct of many industrial processes and can be recompressed and recycled. The process involves a reaction with 100% atom economy and does not involve volatile organic compounds apart from the substrate. There is, therefore, the potential for operating the process as an emissionless synthesis of an important family of commodity chemicals which find use in the manufacture of plasticizers, soaps and detergents.[2]

Acknowledgment. We thank the EPSRC (P.B.W.) and the European Community (TMR program) (M.F.S.) for Fellowships, Sasol for a studentship and secondment (T.E.K.), and the Scottish Higher Education Funding Council, through their Research Development Grant scheme, for funds to purchase the ICPMS instrument. We are also indebted to Robert Cathcart for very considerable input in the reactor development and to Professor K.R. Seddon for a gift of **[BMIM]NTf$_2$**.

Supporting Information Available: An animation showing the operation of the SCF−IL process is provided. This material is available free of charge via the Internet at http://pubs.acs.org.

JA035967S